

The current issue and full text archive of this journal is available on Emerald Insight at:
<https://www.emerald.com/insight/0264-4401.htm>

A three-phase interpenetrating continua approach for wave and porous structure interaction

Wave and
porous
structure
interaction

Liang Yang

Department of Energy and Power, Cranfield University, Bedford, UK

Andrew Buchan

*School of Engineering and Materials Science,
Queen Mary University of London, London, UK*

Dimitrios Pavlidis, Alan Jones and Paul Smith

*Department of Earth Science and Engineering,
Imperial College London, London, UK*

Mikio Sakai

*Resilience Engineering Research Centre, School of Engineering,
The University of Tokyo, Tokyo, Japan, and*

Christopher Pain

*Department of Earth Science and Engineering,
Imperial College London, London, UK*

Received 27 August 2019

Revised 8 March 2020

19 April 2020

Accepted 21 April 2020

Abstract

Purpose – This paper aims to propose a three-phase interpenetrating continua model for the numerical simulation of water waves and porous structure interaction.

Design/methodology/approach – In contrast with one-fluid formulation or multi-component methods, each phase has its own characteristics, density, velocity, etc., and each point is occupied by all phases. First, the porous structure is modelled as a phase of continua with a penalty force adding on the momentum equation, so the conservation of mass is guaranteed without source terms. Second, the adaptive unstructured mesh modelling with PIDG-P1 elements is used here to decrease the total number of degree of freedom maintaining the same order of accuracy.

Findings – Several benchmark problems are used to validate the model, which includes the Darcy flow, classical collapse of water column and water column with a porous structure. The interpenetrating continua model is a suitable approach for water wave and porous structure interaction problem.

Originality/value – The interpenetrating continua model is first applied for the water wave and porous structure interaction problem. First, the structure is modelled as phase of non-viscous fluid with penalty force, so the break of the porous structure, porosity changes can be easily embedded for further complex studies. Second, the mass conservation of fluids is automatically satisfied without special treatment. Finally, adaptive anisotropic mesh in space is employed to reduce the computational cost.

Keywords Fluid-structure interaction, Anisotropic mesh adaptivity, Interpenetrating continua, Porous structure

Paper type Research paper



L. Yang acknowledges support from the EPSRC Grant EP/P013198/1, GCRF from HEFCE/Research England. A. Buchan acknowledges the support from EPSRC Grant EP/M022684/1.

Engineering Computations
© Emerald Publishing Limited
0264-4401
DOI 10.1108/EC-08-2019-0386

Highlights:

- The interpenetrating continua approach for wave and porous structure interaction problem.
 - The porous structure is modelled as a phase of fluid so that the conservation of mass is automatically satisfied in the porous region.
 - Adaptive anisotropic mesh in space is used to reduce the computational cost.
-

1. Introduction

The design, maintenance and protection of the offshore and coastal infrastructures is widely recognised as critically important at national and worldwide levels. Porous structures exert resistant forces on the flow, generate flow energy dissipation in coastal and offshore engineering. Understanding the detailed physical processes of wave interaction with the porous structure and the accurate prediction of the flow processes within and around the porous structure is required. There are many experimental and numerical works on the water wave impact on rigid structures (Blackmore and Hewson, 1984; Dias and Ghidaglia, 2018; Yang *et al.*, 2016; Yang, 2018; Chen *et al.*, 2019) and the deformable structure (Yang *et al.*, 2018), and articulated multibody (Yang *et al.*, 2018). There is few experimental work for the porous structure found in the literature (Lin, 1998; Liu *et al.*, 1999; Santo *et al.*, 2017). Most of the works for the porous structure and water wave interaction are obtained via numerical modelling (del Jesus *et al.*, 2012; Lara *et al.*, 2012; Hu *et al.*, 2012).

For mathematical modelling of the water waves, the most common used Eulerian model is the so-called “one-fluid” approach (Yang, 2015). The computational modelling of water wave is carried out in a similar way to that of the single-phase flow, apart from the consideration of the interface evolution. The interface is fully resolved by interface tracking or capturing methods. The most popular approaches of capturing interface are established by Volume of Fluid (Xie *et al.*, 2014; Pavlidis *et al.*, 2014; Pavlidis *et al.*, 2016) and the Level Set method (Yang *et al.*, 2016; Yang *et al.*, 2018)

Another approach worth mentioning is the particle-based methods, smoothed particle hydrodynamics (SPH) (Shao, 2010; Basser *et al.*, 2017) or moving particle semi-implicit (MPS) (Koshizuka and Oka, 1996; Takabatake *et al.*, 2016; Sun *et al.*, 2019), that has been recently applied to coastal engineering (Shao, 2010; Zhou and Dong, 2018). This approach solves the flow in a Lagrangian framework, solving the kinematics of each particle and its interaction with neighbouring particles. The Lagrangian nature of SPH makes it well suited to simulate free surface flows with rapid changes of the flow field.

There are also simplified wave models, such as non-hydrostatic wave model (Ma *et al.*, 2014) or the potential flow model (Yan and Ma, 2007). The Navier–Stokes equations are greatly simplified, resulting in an explicit equation for free surface evolution. However, this model is not able to simulate the discontinuous free surface, such as breaking waves

The presence of flow through a porous structure is often modelled as a drag and inertia terms with empirical parameters on the macroscopic scale (del Jesus *et al.*, 2012; Lara *et al.*, 2012; Hu *et al.*, 2012). On the other hand, the microscopic approach can fully resolve the flow within the porous structure with the flow resolution being at the pore scale (Yang *et al.*, 2019). However, this requires large computational resources and is impractical for offshore and coastal engineering.

Works prior to the one-fluid approaches include the interpenetrating continua approach which uses an averaged mixture fluid model. Such methods are used extensively in Pain and de Oliveira (1999), chemical reactors (Pain *et al.*, 2001; Pain *et al.*, 2001) and combustion

modellings (Baumgarten, 2006). Different phases or components in a multiple-fluid flow have different fluid properties (e.g. density, viscosity, etc.), and as a result, they move at different velocities, causing relative motions between phases or components. We introduce an interpenetrating model for simulating water wave and porous structure, in which the distribution of different phases or components is represented by their volume fractions and does not rely on continuous tracking of interfaces. The porous structure is fixed by a large penalty drag force added on the structure's inertia term. Another advantage of using the interpenetrating continua model is that the movement, fracture and break of the porous structure, porosity changes can be easily embedded for further complex studies.

The structure of this paper is organised as follows. Section 2 introduces the classical Eulerian conservation laws (conservation of linear momentum and mass) for multiple mixtures of fluids, by considered each fluid separately. Section 3 describes the details of numerical discretisation of the multiphase flow governing equations. An efficient PIDG-P1 scheme set in a Eulerian unstructured mesh is chosen for the spatial discretisation in conjunction with a well-established fractional step method for the fluid-pressure decoupling. Section 4 presents numerical problems, illustrating the capability of the proposed method.

2. Governing equations

Derivation of the interpenetrating continua model can be found in (Temam and Miranville, 2005). In the following, we will write the equation governing the evolution of the mass fractions $\alpha_i, i = 1, \dots, n$.

2.1 Conservation of mass

If there is no mass transfer between each phases.

$$\frac{\partial}{\partial t}(\alpha_i \rho_i) + \nabla \cdot (\alpha_i \rho_i u_i) = 0, \quad 1 \leq i \leq n. \quad (1)$$

Assuming the three phases are all incompressible, we have mass conservation equation:

$$\frac{\partial \alpha_i}{\partial t} + \nabla \cdot (\alpha_i u_i) = 0, \quad 1 \leq i \leq n. \quad (2)$$

Adding up all phases, we have:

$$\nabla \cdot \left(\sum_i^n u_i \right) = 0 \quad (3)$$

which is the global mass conservation equation.

2.2. Conservation of linear momentum

For multiphase problem, the conservation of linear momentum equation can be written as:

$$\alpha_i \rho_i \frac{\partial u_i}{\partial t} + \alpha_i \rho (u_i \cdot \nabla) u_i = -\alpha_i \nabla p_i + \nabla \cdot \sigma'_i + f_i + \alpha_i \rho_i g \quad (4)$$

where $\nabla \cdot \sigma' = \mu_i \Delta^2 u_i + \frac{1}{3} \mu_i \nabla (\nabla \cdot u_i)$ is the viscous force and p is the pressure, f_i is the drag force between phase i and j and will be discussed in Section 2.4.

2.3 Equation of state

In general, to complete the sets of governing equations, it is necessary to introduce an equation of state relating density to pressure. However, in the proposed wave and porous structure interaction model, the three phases are assumed to be incompressible with constant density.

2.4 Inter-phase momentum transfer

The interfacial momentum transfer is crucial to the modelling of multiphase flows. Considered as sources or sinks in the momentum equations, this interfacial force density generally contains the force due to the viscous drag as well as virtual mass and turbulent dispersion which are lumped together as non-drag forces. These interfacial force densities strongly govern the distribution of the volume fraction. The drag forces between the multiple phases are the most important coupling forces.

$$\Sigma_{lg} = \frac{3}{4} C_D \frac{\alpha_{lg} \alpha_{gl} \rho_l |u_g - u_l|}{d_p} \alpha_{lg}^{-2.65} \quad (5)$$

The interfacial drag force components can be modelled according to the interfacial drag force vector f , where u_g , u_l and u_s are unknown variables:

$$f = \begin{cases} \Sigma_{lg}(u_g - u_l) + \Sigma_{sl}(u_s - u_l) & \text{liquid phase} \\ \Sigma_{lg}(u_l - u_g) + \Sigma_{sg}(u_s - u_g) & \text{gas phase} \\ \infty & \text{solid phase} \end{cases} \quad (6)$$

Assume the liquid and solid phase is a continuous phase and air are particulate phase, the inter-facial drag coefficients are [from Ergun equation (Macdonald *et al.*, 1979; Sakai *et al.*, 2014 and Takabatake *et al.*, 2018)], where the first terms is linear with the velocity, corresponding to the viscous effect, the second term in quadratic form of velocity represents the inertia effect:

$$\begin{aligned} \Sigma_{sg} &= 150 \frac{\alpha_{gs}^2 \mu_g}{\alpha_{gs} d_p^2} + 1.75 \frac{\alpha_{gs} \rho_g |u_g - u_s|}{d_p}, \\ \Sigma_{sl} &= 150 \frac{\alpha_{ls}^2 \mu_g}{\alpha_{sl} d_p^2} + 1.75 \frac{\alpha_{gs} \rho_l |u_l - u_s|}{d_p}, \\ \Sigma_{lg} &= \frac{3}{4} C_D \frac{\alpha_{lg} \alpha_{gl} \rho_l |u_g - u_l|}{d_p} \alpha_{lg}^{-2.65} \end{aligned} \quad (7)$$

where d_p is the effective mean particle diameters. For the interfacial drag between liquid and gas phases, the interface drag coefficients based on the correlations by Ishii and Zuber (Ishii and Zuber, 1979) for different flow regimes are normally used for gas-liquid flows. The drag curve C_D can be correlated for individual bubbles across several distinct bubble Reynolds number regions:

$$C_D = \begin{cases} \frac{24}{\alpha_{lg} Re_{lg}} \left[1 + 0.15 (\alpha_{lg} Re_{lg})^{0.687} \right], & \text{if } \alpha_{lg} Re_{lg} \leq 1000 \text{ viscous region} \\ 0.44 & \text{if } \alpha_{lg} Re_{lg} > 1000 \text{ turbulent region} \end{cases} \quad (8)$$

$$Re_{lg} = \frac{\rho_l |u_g - u_l| d_b}{\mu_l} \quad (9)$$

Wave and
porous
structure
interaction

The average bubble diameter is calculated using:

$$d_b = \frac{W_e \sigma}{\rho_l (u_g - u_l)^2}, \quad (10)$$

The normalised volume fraction is calculated as:

$$\alpha_{ij} = \frac{\alpha_i}{\alpha_i + \alpha_j} \quad (11)$$

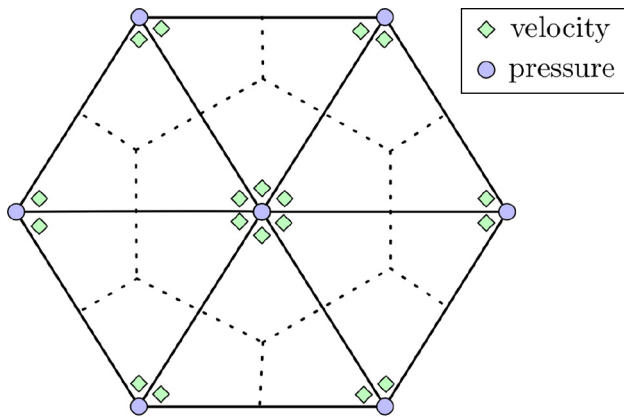
where α_{ij} is the normalised volume fraction of phase i in phase j .

3. Numerical scheme

The spatial discretisation is based on the control volume finite element method. The details of the numerical finite element discretisation and solution of these equations are given (Pavlidis *et al.*, 2014). Here, triangular meshes (2D) tetrahedral (3D) are used to mesh the domain as illustrated in Figure 1. In summary, we use the linear discontinuous between elements velocity and linear continuous pressure (P1DG-P1) for spatial discretisation (Pavlidis *et al.*, 2014). This model has been incorporated into the general purpose CFD code FLUIDITY. A high-order discretisation in time is used based on Crank–Nicholson time stepping. The Courant–Friedrichs–Lewy (CFL) condition is adopted for determining the time step.

4. Numerical examples

In this section, the numerical algorithm and implementation is benchmarked with the experimental data.



Note: The central position of key solution variables (velocity and pressure) are indicated here for the P1DG-P1 pairs in 2 D

Figure 1.
Finite element used to
discretise the
governing equations

4.1 Fluid flow through a porous media

We first benchmark the solver through Darcy flow problem with uniform mesh, where the closure laws for inter-facial momentum is from the Darcy equation. We consider a pipe with the fluid flowing from the inlet (left) to the outlet (right). Half of the pipe is filled with porous media. Geometric parameters are labelled in [Figure 2](#), and specific properties used for the model are listed in [Table 1](#).

As the slip boundary condition is applied to the void space section, the pressure drop is neglected. The analytical pressure drop in the porous media is calculated using the Darcy equation:

$$\frac{q}{A} = v = -\frac{\kappa}{\mu} \frac{dp}{dx} \quad (12)$$

where q is the volumetric flow rate and A is the area of cross section. v is the Darcy velocity, k is the permeability and μ is the viscosity, p is the pressure and x is the coordinate.

The comparison results of the axial pressure with different mesh refinements are shown in [Figure 3](#). It can be seen that the axial pressures of different grid sizes are similar, and the modelling results show good agreements with the analytical solution. Thus, the proposed approach can give relatively accurate results for the modelling of a free flow into the porous media.

4.2 2D collapsing water column

The second numerical example verifies the capability of multi-fluid model for the numerical simulation of free surface flow. The dam break problem is a well-documented example at experimental ([Martin and Moyce, 1952](#)) and numerical ([Yang et al., 2018](#)) level, which simulates the sudden collapse of a square shaped column of water onto a horizontal surface as a result of the effect of gravity. The general description of the problem is presented in [Figure 4](#). For the numerical results presented herein, the side of the (square) water domain is initially prescribed as $a = 1$ m ([Figure 4](#)). The water phase is fully embedded inside a rectangular domain of base length $b = 5$ m, height was chosen as $h = 1.25$ m. Non-slip boundary conditions are considered for all the sides of the rectangular domain. The fluid properties of both phases (water and air) will be referred by the subscripts w and a , respectively) are listed in [Table 2](#).

[Figure 5](#) illustrates a sequence of snapshots of the free surface position as a function of time. Note that an interpenetrating continua model is used, so we take the contour line of volume fraction showing the implicit interface. The predicted heights and the surge front location of the collapsed water are plotted against the dimensionless time $\tau = t \sqrt{h/g}$, as reported in ([Martin](#)

Figure 2.
Schematic of fluid flowing from the void space to the porous media with constant velocity

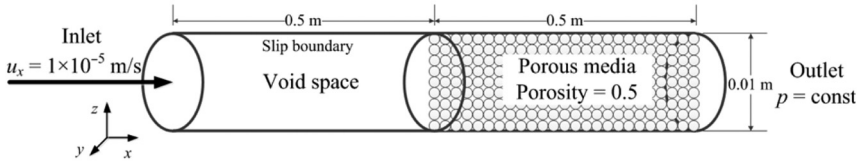


Table 1.
Physical properties used for the modelling

Density	Viscosity	Porosity	Permeability	Outlet pressure	Inlet velocity
1000 kg/m ³	1.0 cp	0.5	0.1	10 ⁵ Pa	10 ⁻⁵ m/s

Wave and porous structure interaction

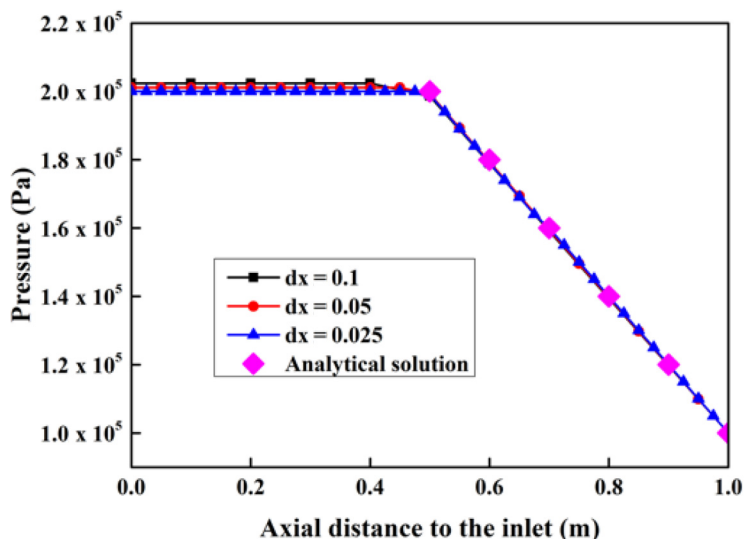


Figure 3. Comparison between the results of mesh refinements and analytical solution

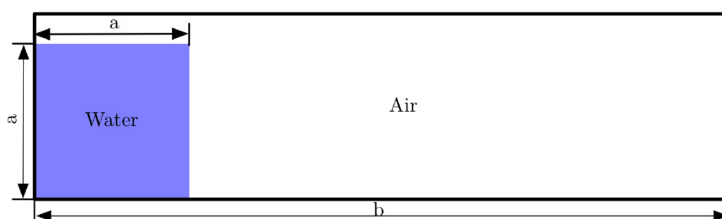


Figure 4. Schematics of the initial conditions for the collapsing water column ($a = 1\text{m}$; $b = 5\text{m}$)

Table 2.

Physical properties of water and air for collapsing water column problem

Water density	Air density	Water viscosity	Air viscosity
$\rho_w = 1000 \text{ kg/m}^3$	$\rho_a = 1 \text{ kg/m}^3$	$\mu_w = 10^{-3} \text{ Pa s}$	$\mu_a = 10^{-5} \text{ Pa s}$

Case 1 (crashed rock)

Case 2 (glass beads)

Table 3.

Computational details of the dam break through a porous structure problem

	Case 1 (crashed rock)	Case 2 (glass beads)
Domain size (m)	$0.89 \times 0.58 \times 0.1$	
Water density (kg/m^3)	1000	
Air density (kg/m^3)	1	
Water viscosity (Pa s)	1×10^{-3}	
Air viscosity (Pa s)	1×10^{-5}	
Baffle position (m)	0.3	
Baffle thickness (m)	0.29	
Average grain size (m)	1.59×10^{-2}	0.3×10^{-2}
Initial dam height (m)	0.25	0.15
Porosity	0.49	0.39

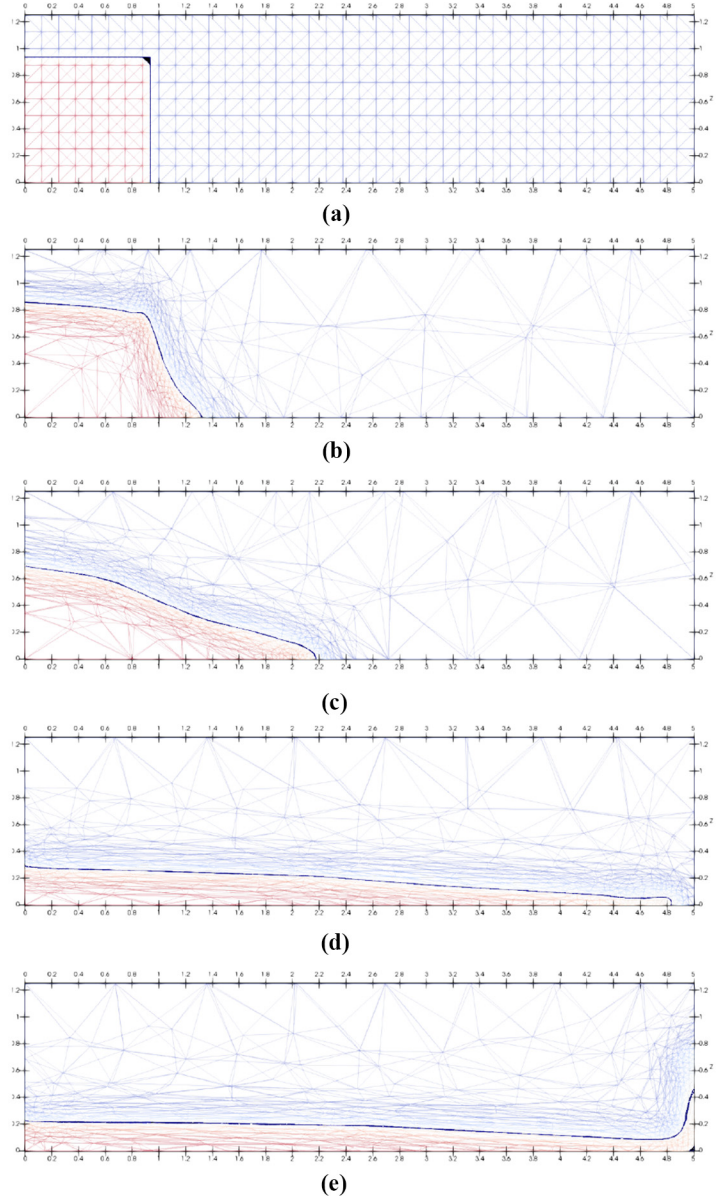
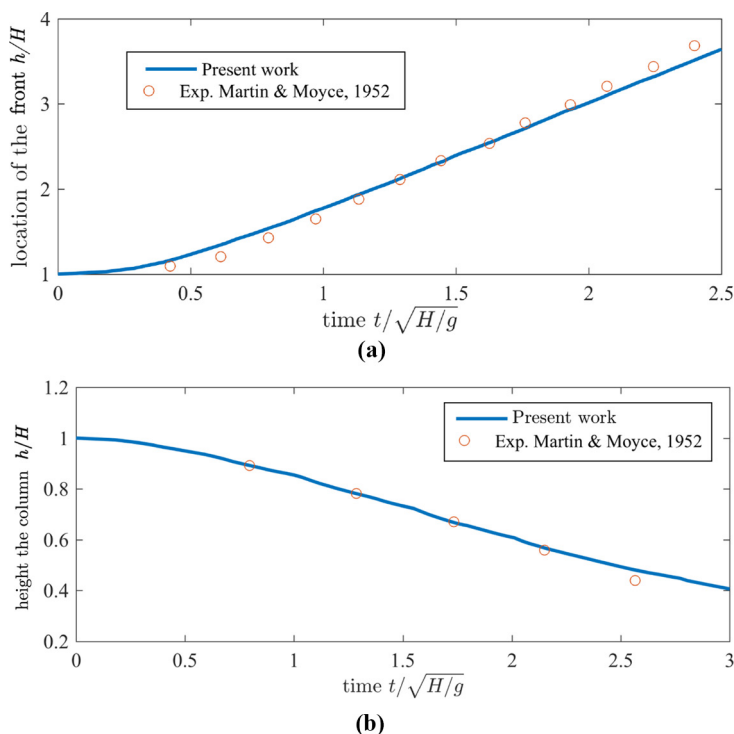


Figure 5.
 Predicted free surface
 evolution at different
 dimensionless time
 steps τ obtained for
 an adaptive mesh

Notes: (a) $\tau = 0.0$; (b) $\tau = 0.6756$; (c) $\tau = 1.4503$; (d) $\tau = 3.8403$;
 (e) $\tau = 4.7086$. The material parameters are as follows: water density
 $\rho_w = 1,000 \text{ kg/m}^3$, air density $\rho_a = 1 \text{ kg/m}^3$, water viscosity $\mu_w = 10^{-3} \text{ Pa s}$,
 air viscosity $\mu_a = 10^{-5} \text{ Pa s}$ (refer to Figure 4 and Table 2)

and Moyce, 1952). In Figure 6, very good agreement can be observed between the numerical simulation obtained using the proposed algorithm and the experimental (Martin and Moyce, 1952) available in the literature. As can be observed, with mesh refinement, the presented results converge extremely well to the latest experimental data.



Notes: (a) Surge front position; (b) water column height. the material parameters are as follows: water density $\rho_w = 1000 \text{ kg/m}^3$, air density $\rho^a = 1 \text{ kg/m}^3$, water viscosity $\mu_a = 10^{-3} \text{ Pa s}$, air viscosity $\mu_a = 10^{-5} \text{ Pa s}$ (Figure 4 and Table 2)

Figure 6. Comparison of the surge front location and the water column height with experimental data and numerical results

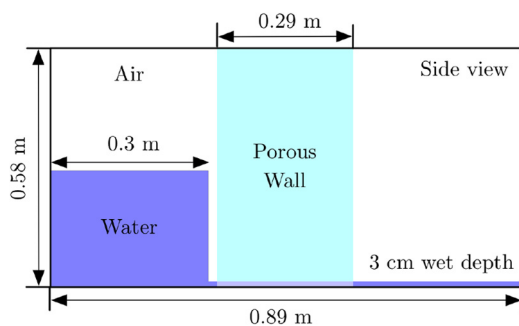


Figure 7. Schematics of the initial condition for the dam break problem

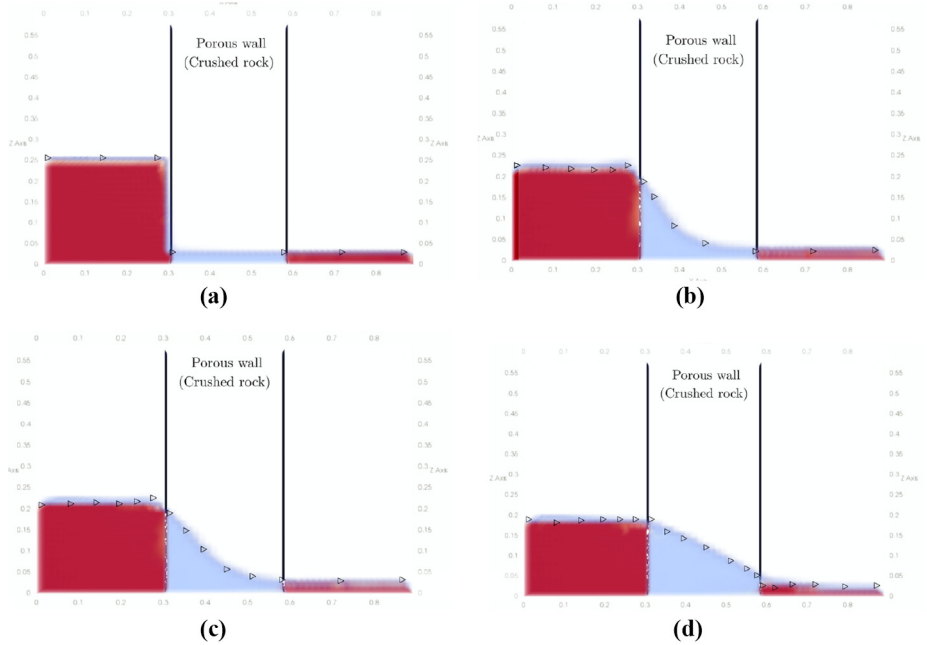


Figure 8.
Comparison of free
surface shapes for
dam break through
crush rock

Notes: (a) $t = 0.00$ s; (b) $t = 0.02$ s; (c) $t = 0.04$ s; (d) $t = 0.12$ s. Triangle markers is from the experimental data by Liu *et al.* (Liu *et al.*, 1999)

Overall, the comparison between the numerical results, the interpenetrating fluid numerical formulation and the experimental date indicate that the present numerical model is capable of simulating the hydrodynamics of water and air.

4.3 2D porous structure and water wave

The second numerical example is performed to verify the drag force by comparing the computational results with the experiment. Lin (1998) tested a dam break wave through different porous materials. The tank is 0.89 m long and 0.555 m height, in the middle there is a porous block of 0.29 m, as shown in Figure 7. Initially, the ground water is 3-cm depth and the water column ext has a 2-cm gap to the left porous wall. Two different baffle materials were used, crushed rocks and glass beads. In Case 1, the porous block is composed by crashed rock with an averaged porosity of 0.49. In Case 2, the glass beads have a porosity of 0.39. The conservation of the mass is guaranteed. There is no “mass loss” compared with the “one-fluid” formulation. The pore-based Reynolds number for the crushed rock experiments is $Re_p = 325$, while for the glass beads experiments it is $Re_p = 9.6$. The physical properties of phases are listed in Table 3.

Figures 8 and 9 show representative snapshots for the two cases. The computed and measured free surface time evolution agrees very well for the two porous media tested.

5. Conclusions

The contribution of this paper is to bring the interpenetrating continua model for modelling the breaking water wave and porous structure interaction. On the basis of

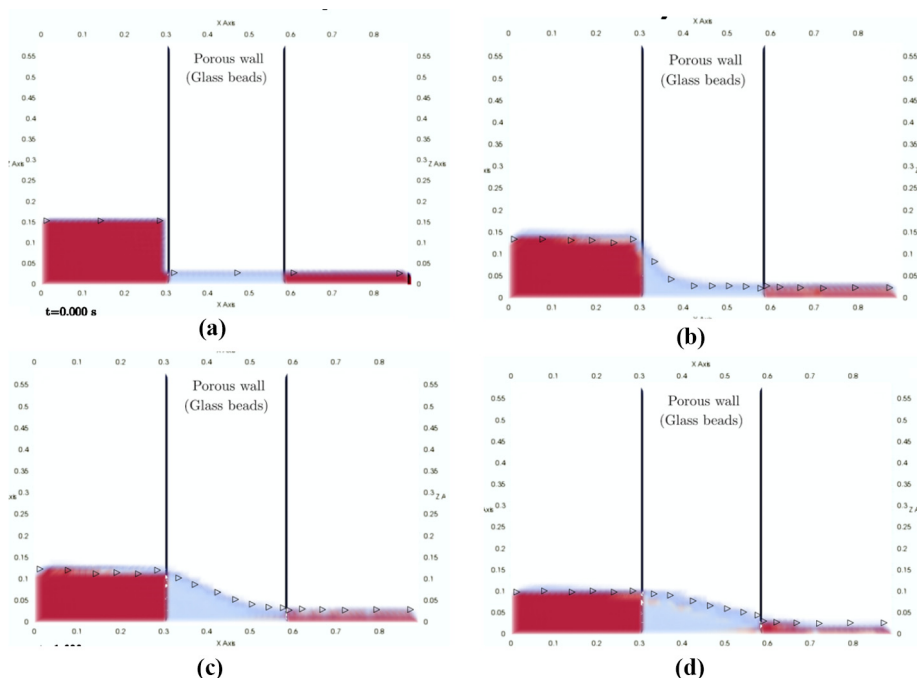


Figure 9. Comparison of free surface shapes for dam break through glass beads barrier

Notes: (a) $t = 0.00$ s; (b) $t = 0.02$ s; (c) $t = 0.04$ s; (d) $t = 0.12$ s. Triangle markers is from the experimental data by Liu *et al.* (1999)

the continua framework, separate transport equations governing the conservation laws are solved for each phase and exchanges that take place at the interfaces are explicitly account for, the dynamics of the interaction between the individual phases can be effectively described via suitable correlation models. These correlation models are well-suited to simulate the macroscopic behaviour of large-scale flows, which do not resolve all the relevant length and timescales. The key success to the application of this model is the reliance on the proper correlation of the inter-phase terms. Several validated cases have been provided in the numerical examples to prove the accuracy of the proposed numerical method.

References

- Basser, H., Rudman, M. and Daly, E. (2017), "SPH modelling of multi-fluid lock-exchange over and within porous media", *Advances in Water Resources*, Vol. 108, pp. 15-28.
- Baumgarten, C. (2006), *Mixture Formation in Internal Combustion Engines*, Springer Science and Business Media.
- Blackmore, P. and Hewson, P. (1984), "Experiments on full-scale wave impact pressures", *Coastal Engineering*, Vol. 8 No. 4, pp. 331-346.
- Chen, L., Stagonas, D., Santo, H., Buldakov, E., Simons, R., Taylor, P. and Zang, J. (2019), "Numerical modelling of interactions of waves and sheared currents with a surface piercing vertical cylinder", *Coastal Engineering*, Vol. 145, pp. 65-83.

-
- del Jesus, M., Lara, J.L. and Losada, I.J. (2012), "Three-dimensional interaction of waves and porous coastal structures: part I: Numerical model formulation", *Coastal Engineering*, Vol. 64, pp. 57-72.
- Dias, F. and Ghidaglia, J.-M. (2018), "Slamming: recent progress in the evaluation of impact pressures", *Annual Review of Fluid Mechanics*, Vol. 50 No. 1, pp. 243-273.
- Hu, K.C., Hsiao, S.C., Hwung, H.H. and Wu, T.R. (2012), "Three-dimensional numerical modeling of the interaction of dam-break waves and porous media", *Advances in Water Resources*, Vol. 47, pp. 14-30.
- Ishii, M. and Zuber, N. (1979), "Drag coefficient and relative velocity in bubbly, droplet or particulate flows", *AIChE Journal*, Vol. 25 No. 5, pp. 843-855.
- Koshizuka, S. and Oka, Y. (1996), "Moving-particle semi-implicit method for fragmentation of incompressible fluid", *Nuclear Science and Engineering*, Vol. 123 No. 3, pp. 421-434.
- Lara, J.L., del Jesus, M. and Losada, I.J. (2012), "Three-dimensional interaction of waves and porous coastal structures: part II: experimental validation", *Coastal Engineering*, Vol. 64, pp. 26-46.
- Lin, P. (1998), *Numerical Modeling of Breaking Waves*, Cornell University.
- Liu, P.L.F., Lin, P., Chang, K.-A. and Sakakiyama, T. (1999), "Numerical modeling of wave interaction with porous structures", *Journal of Waterway, Port, Coastal, and Ocean Engineering*, Vol. 125 No. 6, pp. 322-330.
- Macdonald, I., El-Sayed, M., Mow, K. and Dullien, F. (1979), "Flow through porous media – the ergun equation revisited", *Industrial and Engineering Chemistry Fundamentals*, Vol. 18 No. 3, pp. 199-208.
- Ma, G., Shi, F., Hsiao, S.-C. and Wu, Y.-T. (2014), "Non-hydrostatic modeling of wave interactions with porous structures", *Coastal Engineering*, Vol. 91, pp. 84-98.
- Martin, J.C. and Moyce, W.J. (1952), "An experimental study of the collapse of liquid columns on a rigid horizontal plane", *Philosophical Transactions of the Royal Society of London. Series A, Mathematical and Physical Sciences*, Vol. 244 No. 1, pp. 312-324.
- Pain, C. and de Oliveira, A. (1999), *Goddard, Modelling the Criticality Consequences of Free Surface Motion in Fissile Liquids*, Tech. rep.
- Pain, C., Mansoorzadeh, S. and Oliveira, C.D. (2001), "A study of bubbling and slugging fluidised beds using the two-fluid granular temperature model", *International Journal of Multiphase Flow*, Vol. 27 No. 3, pp. 527-551.
- Pain, C., Mansoorzadeh, S., De Oliveira, C. and Goddard, A.H. (2001), "Numerical modelling of gas–solid fluidized beds using the two-fluid approach", *International Journal for Numerical Methods in Fluids*, Vol. 36 No. 1, pp. 91-124.
- Pavlidis, D., Gomes, J.L., Xie, Z., Percival, J.R., Pain, C.C. and Matar, O.K. (2016), "Compressive advection and multi-component methods for interface-capturing", *International Journal for Numerical Methods in Fluids*, Vol. 80 No. 4, pp. 256-282.
- Pavlidis, D., Xie, Z., Percival, J.R., Gomes, J.L., Pain, C.C. and Matar, O.K. (2014), "Two-and three-phase horizontal slug flow simulations using an interface-capturing compositional approach", *International Journal of Multiphase Flow*, Vol. 67, pp. 85-91.
- Sakai, M., Abe, M., Shigeto, Y., Mizutani, S., Takahashi, H., Viré, A., Percival, J.R., Xiang, J. and Pain, C.C. (2014), "Verification and validation of a coarse grain model of the DEM in a bubbling fluidized bed", *Chemical Engineering Journal*, Vol. 244, pp. 33-43.
- Santo, H., Stagonas, D., Buldakov, E. and Taylor, P. (2017), "Current blockage in sheared flow: experiments and numerical modelling of regular waves and strongly sheared current through a space-frame structure", *Journal of Fluids and Structures*, Vol. 70, pp. 374-389.
- Shao, S. (2010), "Incompressible SPH flow model for wave interactions with porous media", *Coastal Engineering*, Vol. 57 No. 3, pp. 304-316.

- Sun, X., Sun, M., Takabatake, K., Pain, C.C. and Sakai, M. (2019), "Numerical simulation of free surface fluid flows through porous media by using the explicit MPS method", *Transport in Porous Media*, Vol. 127 No. 1.
- Takabatake, K., Mori, Y., Khinast, J.G. and Sakai, M. (2018), "Numerical investigation of a coarse-grain discrete element method in solid mixing in a spouted bed", *Chemical Engineering Journal*, Vol. 346, pp. 416-426.
- Takabatake, K., Sun, X., Sakai, M., Pavlidis, D., Xiang, J. and Pain, C.C. (2016), "Numerical study on a heat transfer model in a Lagrangian fluid dynamics simulation", *International Journal of Heat and Mass Transfer*, Vol. 103, pp. 635-645.
- Temam, R. and Miranville, A. (2005), *Mathematical Modeling in Continuum Mechanics*, Cambridge University Press.
- Xie, Z., Pavlidis, D., Percival, J.R., Gomes, J.L., Pain, C.C. and Matar, O.K. (2014), "Adaptive unstructured mesh modelling of multiphase flows", *International Journal of Multiphase Flow*, Vol. 67, pp. 104-110.
- Yan, S. and Ma, Q. (2007), "Numerical simulation of fully nonlinear interaction between steep waves and 2D floating bodies using the QALE-FEM method", *Journal of Computational Physics*, Vol. 221 No. 2, pp. 666-692.
- Yang, L. (2015), "An immersed computational framework for multiphase fluid-structure interaction", Ph.D. thesis, Swansea University
- Yang, L. (2018), "One-fluid formulation for fluid-structure interaction with free surface", *Computer Methods in Applied Mechanics and Engineering*, Vol. 332, pp. 102-135.
- Yang, L., Gil, A.J., Carreño, A.A. and Bonet, J. (2018), "Unified one-fluid formulation for incompressible flexible solids and multiphase flows: application to hydrodynamics using the immersed structural potential method (ISPM)", *International Journal for Numerical Methods in Fluids*, Vol. 86 No. 1, pp. 78-106.
- Yang, L., Yang, H., Yan, S., Ma, Q. and Bihnam, M. (2016), "Comparative study on water impact problem", in *The 26th International Ocean and Polar Engineering Conference, International Society of Offshore and Polar Engineers*, pp. 27-34.
- Yang, L., Yang, J., Boek, E., Sakai, M. and Pain, C. (2019), "Image-based simulations of absolute permeability with massively parallel pseudo-compressible stabilised finite element solver", *Computational Geosciences*, Vol. 23 No. 5, pp. 881-893.
- Yang, L., Lyu, Z., Yang, P., Pavlidis, D., Fang, F., Xiang, J., Latham, J.-P. and Pain, C. (2018), "Numerical simulation of attenuator wave energy converter using one-fluid formulation", in *The 28th International Ocean and Polar Engineering Conference, International Society of Offshore and Polar Engineers*, pp. 602-607.
- Zhou, Y. and Dong, P. (2018), "A new implementation method of sharp interface boundary conditions for particle methods in simulating wave interaction with submerged porous structure", *Computers and Fluids*, Vol. 177, pp. 87-100.

Corresponding author

Liang Yang can be contacted at: liang.yang@cranfield.ac.uk

For instructions on how to order reprints of this article, please visit our website:

www.emeraldgrouppublishing.com/licensing/reprints.htm

Or contact us for further details: permissions@emeraldinsight.com